

Dynamic Fluorescence Spectroscopy on Single Tryptophan Mutants of EII^{mtl} in Detergent Micelles. Effects of Substrate Binding and Phosphorylation on the Fluorescence and Anisotropy Decay[†]

Dolf Swaving Dijkstra,[‡] Jaap Broos,[‡] Antonie J. W. G. Visser,[§] Arie van Hoek,[§] and George T. Robillard^{*:‡}

Department of Biochemistry, Groningen Biomolecular Sciences and Biotechnology Institute (GBB), University of Groningen, Nijenborgh 4, 9747 AG Groningen, The Netherlands, and Microspectroscopy Centre, Department of Biochemistry, Agricultural University, Dreijenlaan 3, 6703 HA Wageningen, The Netherlands

Received November 25, 1996; Revised Manuscript Received February 17, 1997[⊗]

ABSTRACT: The effects of substrate and substrate analogue binding and phosphorylation on the conformational dynamics of the mannitol permease of *Escherichia coli* were investigated, using time-resolved fluorescence spectroscopy on mutants containing five single tryptophans situated in the membrane-embedded C domain of the enzyme [Swaving Dijkstra et al. (1996) *Biochemistry* 35, 6628–6634]. Since no fluorescent impurities are present in these mutants, the changes in fluorescence and anisotropy could be related with changes in the tryptophan microenvironment. Tryptophans at positions 30 and 42 showed changes in fluorescence intensity decay upon binding mannitol, which were reflected in the changes in lifetime distribution patterns. The disappearance of the shortest-lived decay component in these mutants, as well as in the mutant with a single tryptophan at position 109, indicates a change in the local environment such that quenching via neighboring side chains or solvent is reduced. Phosphorylation at histidine 554 and cysteine 384, located in the cytoplasmic A and B domains of EII^{mtl}, respectively, induced an increase in the average fluorescence lifetimes of all of the tryptophans. The effect was most pronounced for tryptophans 30 and 109 which show large increases in the average fluorescence lifetime mainly due to loss of short-lived decay components. A correlation time distribution of the individual tryptophans deduced from an analysis of the anisotropy decay showed that they differed in their rotational mobility with tryptophan 30 showing the least local flexibility. Phosphorylation resulted in immobilization of W109 which, together with changes in the average fluorescence lifetime, is evidence for a conformational coupling between the phosphorylated B domain and the C domain. The influence of mannitol binding on the rotational behavior of the tryptophans is limited; it induces more internal flexibility at all tryptophan positions. A rotational correlation time of 30 ns was resolved for tryptophan 30, which probably represents a rotational mode of the micelle-embedded C-domain of EII^{mtl} or a portion thereof. Upon phosphorylation, this rotational correlation time increases to 50 ns, probably reflecting a changed spatial orientation of W30 with respect to the C domain. Although kinetic experiments have shown that none of the tryptophans is essential for the catalytic activity of EII^{mtl}, it is significant that the residues most sensitive to mannitol binding, W30 and W42, are both located in the first membrane-spanning α -helix, a portion of which is highly conserved among mannitol-specific EII's of different bacteria.

EII^{mtl} ¹ is the mannitol-specific member of the PTS class of enzymes, which couple the phosphorylation of a carbohydrate to its translocation over the cytoplasmic membrane. It consists of two cytoplasmic domains, IIA^{mtl} and IIB^{mtl}, essential for phosphoryl group transfer to mannitol and one integral membrane-embedded domain, IIC^{mtl}, which is essential for mannitol binding and translocation (Lolkema et al., 1990). All three domains have been separately cloned and purified to homogeneity. The purified domains are still functionally active and can restore complete mannitol phosphorylation activity by complementation (van Weeghel et

al., 1991; Robillard et al., 1993). There is considerable kinetic and binding data on IIC^{mtl} [for reviews, see Lolkema and Robillard (1992) and Postma et al. (1993)], but the structural information on IIC^{mtl} is limited to a proposed topology based on hydrophathy analyses and a *mtlA*–*phoA*

[†] This research has been supported by the Netherlands Foundation for Chemical Research (SON) with financial aid from the Netherlands Organization for the Advancement of Scientific Research (NWO).

* Corresponding author. Telephone: +31 50 3634321. Fax: +31 50 3634165. Email: G. T. Robillard@chem.rug.nl.

[‡] Department of Biochemistry and Groningen Biomolecular Sciences and Biotechnology Institute (GBB), University of Groningen.

[§] Microspectroscopy Centre, Department of Biochemistry, Agricultural University Wageningen.

[⊗] Abstract published in *Advance ACS Abstracts*, April 1, 1997.

¹ Abbreviations: C₁₀E₅, decylpenta(ethylene glycol); cmc, critical micelle concentration; decyl-PEG, decylpoly(ethylene glycol) 300; DOC, sodium deoxycholate; DTT, dithiothreitol; EI, enzyme I of the phosphoenolpyruvate-dependent carbohydrate transport system; EII^{mtl}, the mannitol-specific transporting and phosphorylating enzyme; EII^{mtl}-(Trp-), tryptophan-minus mutant of EII^{mtl}: EII^{mtl}(W30), -(W42), -(W109), and -(W117), EII^{mtl} mutants with tryptophan 30, 42, 109, and 117 each present as a single tryptophan, respectively, while the other three tryptophans had been replaced by phenylalanine; EII^{mtl}-(Trp-)C320WEII^{mtl}, mutant containing a tryptophan only at position 320; EII^{mtl}(Trp-)C384WEII^{mtl}, mutant containing a tryptophan only at position 384; GSH, reduced glutathione; HPr, histidine-containing protein; MEM, maximum entropy method; Mtl, mannitol; PEP, phosphoenolpyruvate; PTF, *p*-terphenyl; PTS, phosphoenolpyruvate-dependent phosphotransferase system; TN, turnover number; Trp, tryptophan.

fusion study (Sugiyama et al., 1991). Tryptophan fluorescence spectroscopy is a valuable technique for obtaining structural and dynamic data especially when mutant proteins containing a single tryptophan residue at different positions are available. In earlier studies, we presented a procedure to isolate EII^{mtl} without fluorescent impurities, using pure detergents and avoiding all contact with plasticizers. This is a prerequisite for reliable tryptophan fluorescence spectroscopy of membrane proteins (Swaving Dijkstra et al., 1996a,b). Data were obtained using steady-state tryptophan fluorescence spectroscopy, supporting the proposed topology of IIC^{mtl} and indicating the possible involvement of the first putative membrane-spanning α -helix of IIC^{mtl} in mannitol binding and/or translocation. The present study presents dynamic data obtained from tryptophan fluorescence intensity and anisotropy decay measurements. In general, the decay in emission intensity is sensitive to the solvation and the specific surroundings of the fluorescent residue (Szabo, 1989) while lifetimes recovered from the decay in fluorescence emission reflect different conformational substates of the tryptophan (Ross et al., 1992; Dahms et al., 1995) and the correlation times recovered from the anisotropy decay reflect segmental rotations of the tryptophan residue, local mobility of part of the peptide chain, or Brownian rotation of the entire protein (Kuipers et al., 1991; Visser et al., 1994). Finally an estimate of the global size and shape is possible from the extreme values of the long correlation times.

MATERIALS AND METHODS

Materials. All water was 3 times distilled in a quartz glass still, filtered, and deionized with a Labconco system (ultrapure water). Sodium deoxycholate (DOC) was obtained from Sigma; C₁₀E₅ was obtained from Kwant High Vacuum Oil Recycling and Synthesis, Bedum, The Netherlands. All C₁₀E₅ and DOC referred to in this paper are purified via crystallization as described (Swaving Dijkstra et al., 1996a,b). Q-Sepharose Fast Flow and S-Sepharose Fast Flow were from Pharmacia (Sweden); hexyl-agarose was from Sigma. D-[1-¹⁴C]Mannitol (59 mCi/mmol; 1 mCi = 37 MBq) was purchased from the Radiochemical Centre Amersham; D-[1-³H(N)]mannitol (976.8 GBq/mmol) was from DuPont NEN Research Products. Enzyme I and HPr were purified as described previously (Dooijewaard et al., 1979; Robillard et al., 1979; van Dijk et al., 1990). All other reagents were analytical grade.

Bacterial Strains and Plasmids: Purification of Single Trp Mutants of EII^{mtl} and EII^{mtl}(Trp-). The bacterial strains and plasmids and the procedure for purification of the mutants to levels where no fluorescent impurities interfered with the tryptophan fluorescence were as published before (Swaving Dijkstra et al., 1996a,b).

Mannitol Phosphorylation Assays. All mutants have been kinetically characterized (Swaving Dijkstra et al., 1996a) by measuring the PEP-dependent mannitol phosphorylation activity as described (Robillard & Blaauw, 1987).

Concentration Determinations on Single Trp Mutants of EII^{mtl} and EII^{mtl}(Trp-). The concentrations of the single Trp mutants of EII^{mtl} and of EII^{mtl}(Trp-) were determined by flow dialysis (Lolkema et al., 1990), assuming one high-affinity binding site ($K_D \sim 100$ nM) per EII^{mtl} dimer.

Viscosity Measurements. The kinematic viscosity (u) was determined at either 4.0 °C or 25.0 °C from the flow time of buffer through a capillary with an internal diameter of

0.46 mm type 525 01/0b, which is suitable for viscosity measurements in the range of 1–5 CSt. The kinematic viscosity (u) can be calculated from

$$u = K(t - \vartheta) \quad (1)$$

where K is the capillary constant (0.005 CSt/s), t is the flow time in seconds, and ϑ is a flow-time-dependent correction in seconds. The dynamic viscosity (η) is related to the kinematic one by

$$\eta = u\rho \quad (2)$$

where ρ is the density of the solution in grams per cubic centimeter.

Fluorescence Measurements. All fluorescence experiments were conducted on samples freshly thawed from liquid nitrogen, containing 0.39–1.2 μ M (0.027–0.082 mg/mL) single Trp EII^{mtl} and EII^{mtl}(Trp-) in 20 mM Tris-HCl, pH 8.4, 1 mM GSH, 300 (± 20) mM NaCl, and 0.25% (v/v) C₁₀E₅, unless stated otherwise. Steady-state fluorescence measurements were performed as described by Swaving Dijkstra et al. (1996b). Time-resolved fluorescence measurements were performed as described elsewhere (Visser et al., 1994; van Hoek et al., 1987). The excitation pulse frequency was reduced to 951.2 kHz, with a pulse duration less than 4 ps. An excitation wavelength of 297 nm was chosen as a golden mean both to ensure efficient excitation of all the different tryptophans and to obtain a high initial anisotropy of the tryptophan residues. Fluorescence emission was selected at 338.9 nm, using a WG320 cutoff filter (Schott, Mainz, Germany) and a Schott 338.9 nm interference filter with a half-width (HW) of 4.8 nm and a maximum transmission (T-max) of 27%. At these emission wavelengths, the single Trp mutants, some of which show highly blue-shifted emissions (Swaving Dijkstra et al., 1996a), still have considerable emission intensities. Experiments were performed at 4 °C, unless stated otherwise. Complete measurements were as described by Pap et al. (1996), using *p*-terphenyl dissolved in cyclohexane/CCl₄ having a fluorescence lifetime of 0.04 ns at 4 °C as reference and EII^{mtl}(Trp-) as background. The fluorescence intensity of EII^{mtl}(Trp-) was between 10 and 40% of the intensity of the single Trp samples. Three different time calibrations were used in the experiments which were 25.0, 30.0, or 40.0 ps/channel, with a total of 1000 channels for each decay curve. One complete measurement consisted of measuring the polarized fluorescence decays of the reference compounds, the sample, the background, and again the reference compound. Reproducibility was found to be satisfactory in duplicate experiments.

Sample Preparations. Mannitol binding experiments were performed with 5 μ M mannitol which was sufficient to ensure over 95% saturation of the binding sites. Perseitol binding was measured at a concentration of 10 μ M, due to a slightly lower affinity for this substrate analogue (Lolkema et al., 1993a). Phosphorylation of EII^{mtl} was accomplished by incubation of the enzyme for at least 5 min at 25 °C in the presence of 5 mM PEP, 5 mM MgCl₂, 1 mM GSH, 0.02 μ M EI, and 1 μ M HPr, just before data acquisition. Iodide quenching was achieved by adding KI to a final concentration of 300 mM, using a stock solution of 3 M KI in water, which contained a trace of Na₂S₂O₃ to prevent formation of I₃⁻. Corrections were made for aspecific effects due to the various

additions by using a background sample of EII^{mtl}(Trp⁻) with the same additions.

Data Analysis. The analysis of the time-dependent decays in fluorescence intensity $I(t)$ and anisotropy $r(t)$ was performed with the commercially available maximum entropy method (MEM, Maximum Entropy Solutions Ltd., U.K.) as described by Bastiaens et al. (1992), Livesey et al. (1987), and Brochon (1994), using starting distributions which were flat in $\log(\tau)$ and $\log(\phi)$ space. The χ^2 values were close to 1.0 for all data sets. The weighted residuals between experimental and calculated decay curves and the autocorrelation function of the residuals (Vos et al., 1987) were randomly distributed around zero, indicating optimal fits. The total anisotropy decay consisting of i different internal tryptophan rotations as well as total protein rotations is given by:

$$r(t) = \left\{ \sum_i \beta_i \exp(-t/\phi_i) + \beta_{\text{prot}} \right\} \exp(-t/\phi_{\text{prot}}) \quad (3)$$

When the different ϕ_i 's are much shorter than ϕ_{prot} , the MEM resolved short correlation times are very close to the actual ϕ_i 's. The preexponential factors are related to the so-called order parameter S for the tryptophan residue, via:

$$S^2 = \beta_{\text{prot}} / (\sum_i \beta_i + \beta_{\text{prot}}) \quad (4)$$

In the absence of internal tryptophan motion ($\sum_i \beta_i = 0$), the tryptophan only rotates together with the protein and S equals unity. In the case of internal flexibility of the tryptophan, the order parameter is related to the angular displacement, ψ , of the motion, via:

$$S^2 = 0.5 \cos \psi (\cos \psi + 1) \quad (5)$$

The correlation time of the Brownian rotation of a protein (ϕ_{prot}) depends on the hydrated volume (V) and shape of the protein (or protein-detergent complex), as well as on the temperature (T) and viscosity (η) of the solution as given by the Stokes-Einstein equation (spherical particle):

$$\phi_{\text{prot}} = \eta V / kT = M(\hat{u} + h)\eta / RT \quad (6)$$

where k is the Boltzmann constant, M is the molecular mass of the protein, \hat{u} is the partial specific volume (milliliters per gram), and h the amount of hydration (milliliters per gram) of the rotating particle. Deviations from the expected ϕ_{prot} can be the result of a nonspherical shape.

RESULTS

Fluorescence Decay of Mutants of EII^{mtl}. Multiple fluorescence lifetimes are necessary to adequately describe the fluorescence decays of the different single tryptophan mutants of EII^{mtl} (Table 1). A typical example of the fluorescence decay together with the lifetime distribution resolved by a MEM analysis is shown in Figure 1, for EII^{mtl}(W30). The residuals and the autocorrelation function indicate that the trimodal distribution of lifetimes with barycenters located at 0.15, 1.26, and 4.02 adequately describes the experimental decay. There is also a small contribution (<2%) of a long-lived decay component of 19.9 ns, which is found repeatedly in different preparations of this mutant. Extremely short lifetimes of 0.07–0.15 ns, indicative of the presence of strongly quenched substates of the tryptophan residues, were present in all mutants except W320.

Table 1: Effects of Mannitol Binding and Phosphorylation on the Total Intensity Decay Parameters of Mutants of EII^{mtl} ^a

	c_1	c_2	c_3	c_4	τ_1 (ns)	τ_2 (ns)	τ_3 (ns)	τ_4 (ns)	$\langle \tau \rangle$ (ns)
W30	0.10	0.46	0.42	0.02	0.14	1.2	4.0	20	2.6
+mtl		0.70	0.30			2.5	5.0		3.3
+P		0.39	0.59	0.02		1.2	3.7	18	3.0
W42	0.06	0.18	0.23	0.53	0.13	0.61	2.6	5.9	3.8
+mtl		0.11	0.17	0.72		0.74	2.8	6.1	4.9
+P	0.05	0.14	0.20	0.61	0.15	0.57	2.1	5.7	4.0
W109	0.11	0.19	0.33	0.37	0.13	0.60	2.3	5.7	3.0
+mtl		0.26	0.37	0.37		0.55	2.2	5.8	3.1
+P			0.37	0.63			2.1	5.2	4.0
W117	0.14	0.23	0.34	0.29	0.07	0.62	2.5	5.6	2.6
+mtl	0.13	0.20	0.35	0.32	0.12	0.67	2.4	5.4	2.7
+P	0.15	0.20	0.33	0.32	0.11	0.59	2.4	5.5	2.7
W320		0.16		0.83		1.0		4.8	4.2
+mtl		0.10	0.27	0.63		0.86	2.4	5.5	4.2
+P		0.22		0.78		1.7		5.2	4.4

^a The total intensity decay was assumed as $I(t) \sum_i c_i \exp(-t/\tau_i)$. τ values are the barycenters of each lifetime class, and c values are the normalized areas over each class.

Effect of Mannitol and Perseitol Binding and Phosphorylation on Fluorescence Decay of Mutants of EII^{mtl}. Table 1 shows that mannitol binding induces changes in the fluorescence lifetimes especially of W30 and W42, which are both predicted in the first putative membrane-spanning α -helix of the C domain (see Figure 2). The average fluorescence lifetimes, $\langle \tau \rangle$, increase from 2.6 to 3.3 ns and from 3.8 to 4.9 ns for W30 and W42, respectively. Mannitol binding specifically seems to eliminate the short-lived component, τ_1 , which is about 0.14 (± 0.01) ns in W30, W42, and W109, suggesting a loss of a strongly quenched tryptophan conformer in these mutants. The binding of perseitol induced similar changes.

Phosphorylation of the single tryptophan mutants at H554 and C384 in the A and B domains, respectively, also led to changes in average lifetimes which were most pronounced for W30 and W109. The short-lived component in these mutants was again eliminated, resulting in longer average fluorescence lifetimes. For W30, the average lifetime increased from 2.6 to 3.0 ns, while for W109 the increase was from 3.0 to 4.0 ns. W109 loses both sub-nanosecond lifetimes, resulting in a biexponential decay with fluorescence lifetimes of 2.1 and 5.2 ns.

Effect of Iodide Quenching on the Fluorescence Decay of Mutants of EII^{mtl}. Table 2A and 2B list the fluorescence lifetimes and quenching parameters, respectively, for the quenching of the single Trp mutants by 300 mM potassium iodide. Quenching rate constants, k_q , of $0.05 \times 10^9 \text{ M}^{-1} \text{ s}^{-1}$ (W30), $0.16 \times 10^9 \text{ M}^{-1} \text{ s}^{-1}$ (W42), and $0.13 \times 10^9 \text{ M}^{-1} \text{ s}^{-1}$ (W320) indicate buried positions of these tryptophans, whereas the tryptophans in W109 and W117 are more solvent-exposed, having k_q 's of $0.34 \times 10^9 \text{ M}^{-1} \text{ s}^{-1}$ and $0.56 \times 10^9 \text{ M}^{-1} \text{ s}^{-1}$, respectively. All constants are considerably smaller than the bimolecular collision constant (k_c) between iodide and a completely exposed tryptophan in a protein which is about $3.7 \times 10^9 \text{ M}^{-1} \text{ s}^{-1}$ in the buffer at 4 °C (Eftink & Ghiron, 1976). Mannitol binding results in increased fluorescence intensities for W30, W42, W109, and W117 in the presence of iodide. Table 2A shows the effects of mannitol binding on the distributed and average lifetimes in the presence of iodide. All mutants except W320 have longer average fluorescence lifetimes upon mannitol binding, as was the case in the absence of iodide. Table 2B shows the

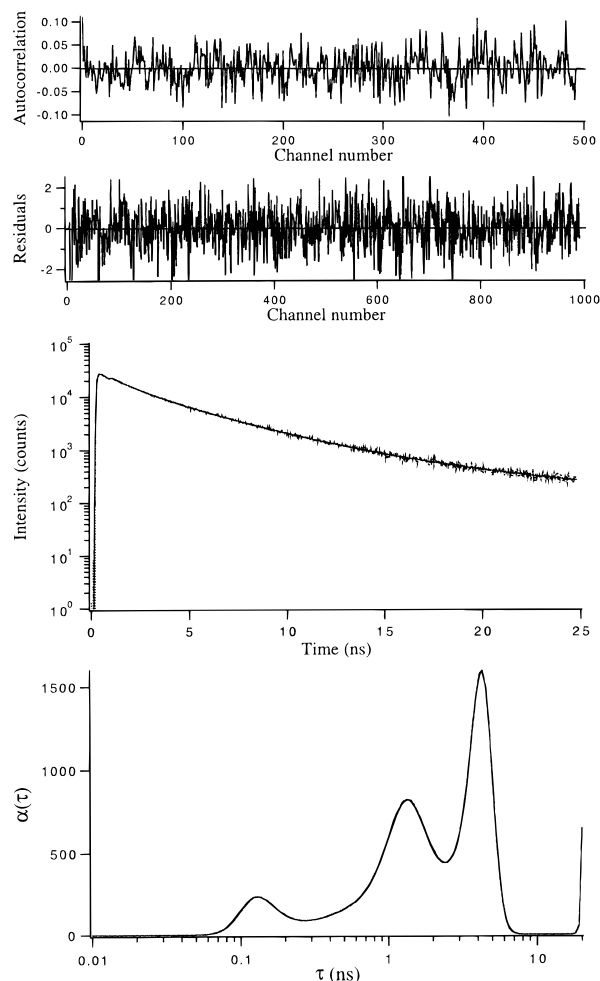


FIGURE 1: Experimental and fitted fluorescence decays of EII^{mtl} (W30) in 20 mM Tris-HCl, pH 8.4, 300 (± 20) mM NaCl, 0.25% C₁₀E₈, and 1 mM GSH at 4 °C (center panel). The bottom panel shows the MEM-resolved lifetime distribution. The two top panels show the weighted residuals between the experimental and fitted curves and the autocorrelation function of the residuals ($\chi^2 = 1.075$). The time-equivalence per channel is 25 ps. The analysis of the barycenters in the lifetime distribution yielded 0.15 ± 0.06 ns, 1.26 ± 0.19 ns, 4.02 ± 0.25 ns, and 19.9 ± 1.2 ns, respectively. The analysis of the amplitudes yielded 0.10 ± 0.04 , 0.45 ± 0.08 , 0.43 ± 0.07 , and 0.019 ± 0.002 , respectively.

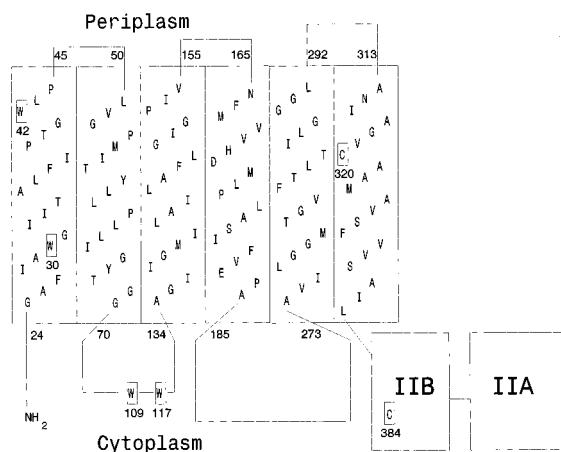


FIGURE 2: A 2D representation of the membrane disposition of the C domain of EII^{mtl} (Sugiyama et al., 1991). The C domain residue positions investigated in this study, 30, 42, 109, 117, and 320, and position 384 in the B domain are enclosed in boxes.

quenching parameters in the absence and presence of mannitol. For W42, a decrease in K_{SV} from 0.63

Table 2A: Effect of Iodide Quenching on Total Intensity Decay Parameters of Several Mutants of EII^{mtl} ^a

	c_1	c_2	c_3	c_4	τ_1 (ns)	τ_2 (ns)	τ_3 (ns)	τ_4 (ns)	$\langle \tau \rangle$ (ns)
W30	0.10	0.46	0.42	0.02	0.14	1.2	4.0	nr	2.6
+I ⁻		0.29	0.70	0.01		0.69	3.1	16	2.5
+I ⁻ /mtl		0.25	0.74			1.1	3.5		2.9
W42	0.06	0.18	0.23	0.53	0.13	0.61	2.6	5.9	3.8
+I ⁻	0.05	0.22	0.21	0.52	0.21	0.56	2.0	5.1	3.2
+I ⁻ /mtl		0.14	0.17	0.69		0.72	2.3	5.5	4.3
W109	0.11	0.19	0.33	0.37	0.13	0.60	2.3	5.7	3.0
+I ⁻		0.36	0.63	0.01		0.60	3.2	17	2.3
+I ⁻ /mtl		0.15	0.37	0.48		0.89	1.2	3.9	2.4
W117	0.14	0.23	0.34	0.29	0.07	0.62	2.5	5.6	2.6
+I ⁻	0.10	0.30	0.37	0.23	0.22	0.58	1.8	4.2	1.8
+I ⁻ /mtl	0.11	0.30	0.37	0.23	0.20	0.63	2.0	4.3	1.9
W320		0.16		0.83		1.0		4.8	4.2
+I ⁻		0.13	0.20	0.66		0.88	1.8	4.6	3.6
+I ⁻ /mtl		0.24	0.52	0.23		1.1	3.5	5.6	3.4

^a The total intensity decay was assumed as $I(t) \sum_i c_i \exp(-t/\tau_i)$. τ values are the barycenters of each lifetime class, and c values are the normalized areas over each class. I⁻ concentrations were 300 mM.

Table 2B: Parameters for Iodide Quenching of Single Trp Mutants of EII^{mtl} ^a

	$K_{SV}(\text{time-resolved})$ (M ⁻¹)	k_q (M ⁻¹ s ⁻¹)	p	$K_{SV}(+mtl)$ (TR) (M ⁻¹)
W30	0.13	0.05×10^9	1/74	0.46
W42	0.63	0.16×10^9	1/23	0.47
W109	1.0	0.34×10^9	1/11	0.97
W117	1.5	0.56×10^9	1/6.6	1.4
W320	0.56	0.13×10^9	1/28	0.78

^a K_{SV} values were determined using $\langle \tau \rangle_0 / \langle \tau \rangle_q = 1 + K_{SV}[Q]$. k_q was obtained from $K_{SV} = k_q \langle \tau \rangle_0$, and the probability for deactivation (p) from $k_q = pk_c$, where k_c is the bimolecular collisional rate constant between iodide and an exposed protein-associated tryptophan. $\langle \tau \rangle$'s from Tables 1 and 2A were used.

M⁻¹ was observed, whereas for W30 and W320, K_{SV} increases from 0.13 to 0.46 M⁻¹ and from 0.56 to 0.78 M⁻¹, respectively. For W109 and W117, no significant changes in quenching constants were observed upon addition of mannitol.

Rotational Behavior of the Different Tryptophan Residues.

Figure 3 shows the experimental decay in anisotropy and the result of a MEM analysis of this decay for EII^{mtl}(W30). The residuals and the autocorrelation function indicate that two rotational correlation times (ϕ) adequately describe the experimental decay. The rotational correlation times for all single Trp mutants are listed in Table 3. They can be classified as high-frequency Trp internal/segmental rotation (ϕ_{int} : ϕ_1, ϕ_2) differing strongly per mutant, and low-frequency motions of a larger portion of the enzyme (ϕ_{prot} : ϕ_3), which is only properly resolved for EII^{mtl}(W30). A rotational correlation time of 30 (± 4) ns was recovered repeatedly for different preparations of EII^{mtl}(W30) at 277 K and a viscosity of 1.67 cP. All of the single Trp mutants show limited internal motion of the tryptophan residue, as can be seen from large values of the order parameter (S). S varies from 0.97 (W30) to 0.90 (W109), indicating that W30 is almost immobilized in the protein, having an angular displacement (ψ) of only 15°, while W109 has somewhat more internal motion reflected by its angular displacement of 30°.

Effects of Mannitol Binding and Phosphorylation on the Rotational Behavior of Tryptophan Residues in EII^{mtl}. From Table 3, it can be seen that upon mannitol binding the single segmental rotations of the tryptophans in W109 and W117,

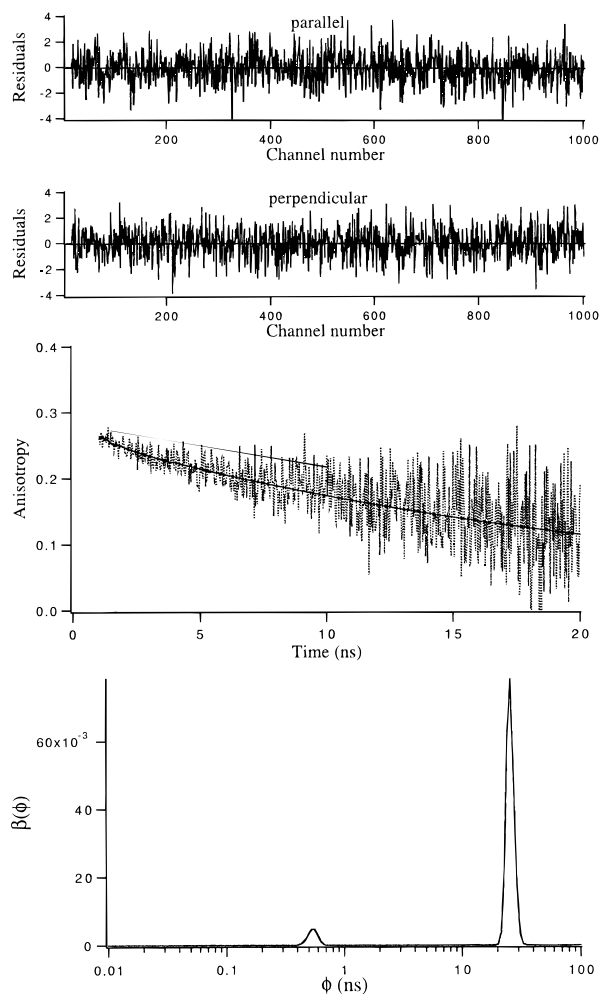


FIGURE 3: Reconstructed experimental and fitted fluorescence anisotropy decays of EII^{mtl}(W30) in 20 mM Tris-HCl, pH 8.4, 300 (± 20) mM NaCl, 0.25% C₁₀E₅, and 1 mM GSH at 4 °C (center panel, the first 40 and last 190 channels were omitted for clarity). The time-equivalence per channel is 25 ps. The bottom panel shows the MEM-resolved correlation time distribution. The two top panels show the weighted residuals between the experimental and fitted curves for the parallel and perpendicular intensity components, respectively ($\chi^2 = 1.337$). The analysis of the barycenters in the correlation time distribution yielded 0.53 ± 0.18 ns and 25.6 ± 0.8 ns, respectively. The analysis of the amplitudes yielded 0.019 ± 0.005 and 0.241 ± 0.002 , respectively.

with correlation times of 1.3 and 1.7 ns, respectively, are both split up into two separate rotational modes of 0.44 and 2.5 ns for W109 and 0.69 and 2.2 ns for W117. Furthermore, for all mutants, the order parameter (S) slightly decreases by mannitol binding.

Phosphorylation does not induce changes in the internal rotational modes of tryptophan in all five mutants. However, it decreases the angular freedom of W30, W42, and W109, whereas the angular freedom for W117 and W320 is increased (Table 3). The effect of phosphorylation is most pronounced for W109, which shows an increase in S of 0.90–0.97. W30 shows an increase in the long rotational correlation time from 30–51 ns, when this mutant is phosphorylated.

DISCUSSION

Excited State Lifetime Distribution of Single Trp Mutants of EII^{mtl}. A MEM analysis of the fluorescence intensity decays of five different tryptophans revealed the existence of 2–4 discrete components for each residue, each represent-

Table 3: Effects of Mannitol Binding and Phosphorylation on the Fluorescence Anisotropy Parameters of Mutants of EII^{mtl} ^a

	β_1	β_2	β_3	ϕ_1 (ns)	ϕ_2 (ns)	ϕ_3 (ns)	S	ψ (deg)
W30	0.013		0.24	0.73 (0.23)		30 (16)	0.97	15
+mtl	0.020		0.29	0.31 (0.04)		26 (5.5)	0.96	17
+P	0.010		0.25	1.3 (0.23)		51 (22)	0.98	13
W42	0.009	0.036	0.20	0.94 (0.17)	3.0 (0.43)	nr	0.91	29
+mtl	0.005	0.048	0.19	0.56 (0.05)	4.0 (0.44)	nr	0.88	32
+P	0.005	0.030	0.21	0.70 (0.15)	2.2 (0.36)	nr	0.93	26
W109	0.047		0.20	1.3 (0.05)		nr	0.90	30
+mtl	0.025	0.036	0.19	0.44 (0.11)	2.5 (0.51)	nr	0.87	34
+P	0.014		0.24	1.7 (0.08)		nr	0.97	16
W117	0.034		0.21	1.7 (0.13)		nr	0.93	25
+mtl	0.016	0.022	0.21	0.69 (0.22)	2.2 (0.68)	nr	0.92	27
+P	0.038		0.21	1.5 (0.13)		nr	0.92	26
W320	0.038	0.002	0.21	1.7 (0.49)	4.7 (0.88)	nr	0.92	27
+mtl	0.044		0.20	2.2 (0.34)		nr	0.91	29
+P	0.049		0.21	2.2 (0.27)		nr	0.90	30

^a The anisotropy decay is described by: $r(t) = \{\sum_i \beta_i \exp(-t/\phi_i) + \beta_3\} \exp(-t/\phi_3)$, where β 's are determined from the integrated curves of the correlation time distributions and ϕ 's are determined from the barycenters. Values in parentheses are the half-widths. The value of $r(0)$ equals $\sum_i \beta_i$. S and ψ are determined from eqs 4 and 5, respectively. nr means not resolved and implies a correlation time > 100 ns.

ing a different substate of the tryptophan residue whose fluorescence is quenched to a certain extent. Short fluorescence lifetimes of 0.07–0.15 ns indicate highly deactivated substates generated by processes such as excited-state reactions, dynamic quenching, and energy transfer to nearby amino acids. Residues like aspartate, glutamate, histidine, tyrosinate, and cysteine can act as quenchers of tryptophan fluorescence provided that they are in van der Waals contact. There is too little information on the global architecture of EII^{mtl} to speculate on the residues responsible for this quenching.

Rotational Behavior of the Tryptophan Residues in Single Trp Mutants of EII^{mtl}. The MEM analysis reveals that the bulk of the experimental anisotropy decay is associated with low-frequency motions. β_3 values in Table 3, which express the contribution of these motions, account for 81–95% of the total decay. With the exception of W30, the correlation times of the low-frequency motions (ϕ_3) cannot be resolved properly since they are too long relative to the lifetimes of the tryptophans. High-frequency motions with variations in correlation times from 0.3 to 4.7 ns probably represent internal and/or segmental motions of the tryptophan residues. The contribution of these high-frequency motions to the anisotropy decay, however, is limited. This is evident from the large values of the order parameters (S), which are ≥ 0.90 for all mutants, indicative of highly immobilized tryptophan residues. The presence of two different high-frequency motions for a single tryptophan could be due to the tendency of MEM to generate additional components; global analysis of the anisotropy decay results in these cases in a single high-frequency component which is about the average of the two original components.

Fluorescence Details of Single Tryptophan Residues in EII^{mtl}. Detailed analysis of the fluorescence characteristics of the individual tryptophans in mutants of EII^{mtl} provides site-specific information on the influence of phosphorylation and substrate binding. W30 is by far the least accessible tryptophan, with a probability of deactivation (p) of 1/74. It is most likely located in the hydrophobic confines of the first membrane-spanning α -helix in the C-domain as indicated by a largely blue-shifted emission maximum at 324

nm (Swaving Dijkstra et al., 1996a). Mannitol binding results in the loss of a short-lived lifetime, causing a change in the distribution of lifetimes and an increase in the average lifetime. These trends are also seen upon phosphorylation of the cytoplasmic A and B domains. These observations indicate that phosphorylation and mannitol binding induce the removal of a deactivation path either by blocking the solvent accessibility of W30 or by removal of a local quencher. Since mannitol binding increases the K_{sv} for I^- quenching at W30, it obviously makes W30 more accessible to components in the solvent. Therefore, we must conclude that the mannitol-induced changes in lifetime reflect the loss of a local quencher by the rearrangement of one or more neighboring side chains.

The anisotropy decay of W30 can be described by a small component of high-frequency oscillation describing an angular motion of approximately 15° , and a larger component describing the motion of the whole C domain or some segment of it. Both ϕ 's are reduced upon mannitol binding, the high-frequency component by more than a factor of 2 and the low-frequency component only slightly. Phosphorylation, on the other hand, increases both the low- and high-frequency components by a factor of 2. The changes in ϕ_1 , the high-frequency internal tryptophan motions, indicate changes in the local environment, whereas the change in ϕ_3 could be due to a change in the spatial orientation of W30 with respect to the rotational axes of the C domain or some flexible segment of the C domain. For an asymmetrical unit containing a strongly immobilized fluorophore, the correlation time which is found depends on the orientation of the excited dipole with respect to the rotational axes. In summary, the fluorescence data on W30 indicate a largely immobilized residue buried in a hydrophobic environment, which is sensitive to mannitol binding and phosphorylation. Mannitol binding loosens up this portion of the structure, increasing side chain flexibility and inducing somewhat more solvent exposure, whereas phosphorylation of the cytoplasmic domains seem to influence the spatial orientation of this residue located in the membrane-embedded domain.

Although W30 and W42 are most likely located in the first membrane-spanning α -helix, and are sensitive to mannitol binding and phosphorylation, the fluorescence characteristics of both residues differ. W42 is more solvent-accessible than W30, possessing a probability of deactivation of 1/23 and an emission maximum of 337 nm versus 1/74 and 324 nm for W30. As with W30, mannitol binding causes the elimination of a short-lived lifetime component, but, in contrast to W30, mannitol binding results in a decreased accessibility of W42. This restriction to I^- and, thus, solvent accounts for the disappearance of the short-lived component in the fluorescence decay. Phosphorylation induces comparable changes in the lifetimes of W42 and W30, although the short-lived component of W42 is not completely eliminated. The anisotropy decay of W42 is composed of two separate high-frequency motions and a nonresolvable low-frequency rotation. A contribution of internal rotations to the total anisotropy decay is indicated by an order parameter of 0.91, corresponding to an angular displacement of 29° . Upon mannitol binding, the angular displacement of the internal motion of W42 increases somewhat to 32° , whereas upon phosphorylation it decreases to 26° .

W109 shows the fluorescence characteristics of a more solvent-exposed tryptophan, possessing a fluorescence emission maximum of 340 nm and a probability of deactivation

of 1/11. This is in line with its expected location in a structure at the cytoplasmic side connecting helices 2 and 3. Mannitol binding does not result in considerable changes in fluorescence intensity, average fluorescence lifetime, or solvent exposure of W109, though the short-lived component of the intensity decay disappears. On the other hand, phosphorylation leads to a large increase in the average fluorescence lifetime and disappearance of the two shortest lived decay components. This is spectroscopic evidence for a conformational coupling between the phosphorylation state of the cytoplasmic A and B domains and the membrane-bound C domain in EII^{mtl}. This coupling is also seen from the changes in anisotropy decay of W109 induced by phosphorylation; the limited internal mobility of W109 is highly restricted by phosphorylation, resulting in an angular displacement of only 16° .

W117 is the most solvent-exposed of all different tryptophans in EII^{mtl}. It has a probability of deactivation of 1/6.6 and an emission maximum of 339 nm. Like the other tryptophans, it is highly immobilized and possesses short-lived decay components. However, none of the fluorescence characteristics of this tryptophan change significantly upon mannitol binding or phosphorylation.

The tryptophan at position 320 replaces a naturally occurring cysteine. Though this cysteine is not conserved among the various mannitol-specific EII's (Figure 4), it is able to report on the conformational changes occurring upon phosphorylation, since it becomes accessible for cysteine-specific reagents when C384 is phosphorylated (Roossien et al., 1984). Kinetic data (Swaving Dijkstra et al., 1996a) and the present fluorescence data indicate that this position is not important for mannitol binding or phosphorylation. W320 has a fluorescence emission maximum (330 nm) and quenching characteristics (p : 1/28) which are in line with its expected location in a membrane-spanning α -helix. The fluorescence decay does not contain short-lived components like the other tryptophans; the average fluorescence lifetime of W320 is the longest of all tryptophans investigated in this study. The long lifetime and an emission intensity which is significantly higher than the other tryptophans suggest very little participation by neighboring residues in the deactivation of the excited state of this tryptophan. The limited solvent exposure slightly increases with mannitol binding, which introduces a separate lifetime as well.

General Conclusion. W30 and W42, both situated in the first putative membrane-spanning α -helix, experience the largest increase in $\langle\tau\rangle$ upon mannitol binding. This is in accordance with the increased fluorescence intensities of these mutants in the steady-state fluorescence analysis (Swaving Dijkstra et al., 1996a). Since both tryptophans have been removed without a substantial change in the K_D for mannitol, the change in lifetimes must be signalling an indirect rather than a direct response to mannitol binding. Thus far, all residues thought to be essential for mannitol binding have been located in the large cytoplasmic "loop" between helix 4 and helix 5 (Manayan et al., 1988; Weng et al., 1992; Briggs et al., 1992). Interestingly, regions of this loop and the first helix are highly conserved among different members of the PTS carbohydrate transporters (Lengeler et al., 1990, 1994; Henstra et al., 1996).

Phosphorylation of H554 and C384 located in the A and B domains of EII^{mtl}, respectively, induced changes in the fluorescence lifetimes which were most pronounced for W30 and W109 in the C domain. It also caused a decreased

internal flexibility for W109 and an increase in the long correlation time of W30. These changes indicate a coupling between the phosphorylation state of the cytoplasmic domains of EII^{mtl} and the physical properties of some residues in IIC^{mtl}, analogous to the coupling between these domains reported in kinetic studies of Lolkema et al. (1991) and Boer et al. (1995).

It is possible that the loop containing W109 forms part of the B/C domain interface. All tryptophans are highly immobilized, with angular displacements (ψ) associated with the internal motions varying from 15° (W30) to 30° (W109). The total anisotropy decay was properly resolved only for W30; a low-frequency motion with a correlation time of 32 (± 3) ns was repeatedly found. Since this correlation time is too short to represent motions of the EII^{mtl} dimer in detergent, which has a molecular mass (enzyme plus detergent) of at least 160 kDa and an expected correlation time, in the case of a spherical shape, of 120–140 ns [via (6), assuming a partial specific volume (\bar{v}) of 0.74 mL/g and a hydration of 0.30 mL/g], it seems likely that it corresponds to the motion of a monomeric IIC^{mtl} unit, or a portion thereof. The absence of a 30 ns correlation time in the other single Trp mutants could be due to different spatial orientation of the tryptophans such that only W30 is orientated properly to resolve the 30 ns rotational mode. Other rotational modes, about different axes, could be too slow to be resolved using tryptophan fluorescence. Mannitol binding does not significantly change the long correlation time of W30, indicating no change in the shape of IIC^{mtl} or in the spatial orientation of the tryptophans examined. Other single tryptophan mutants are being constructed to expand these studies to the region of IIC^{mtl} not covered in the present investigation.

ACKNOWLEDGMENT

We acknowledge Berent Kwant for his assistance during viscosity measurements, S. A. Henstra for the sequence alignment, and J. S. Lolkema, H. Enequist, and W. Minke for the construction of the genes encoding the mutants.

REFERENCES

- AB, E., Schuurman-Wolters, G. K., Saier, M. H., Reizer, J., Jacuinod, M., Roepstorff, P., Dijkstra, K., Scheek, R. M., & Robillard, G. T. (1994) *Protein Sci.* 3, 282–290.
- Akagawa, E., Kurita, K., Sugawara, T., Nakamura, K., Kasahara, Y., Ogasawara, N., & Yamane, K. (1995) *Microbiology* 141, 3241–3245.
- Bastiaans, P. I. H., van Hoek, A., Benen, J. A. E., Brochon, J. C., & Visser, A. J. W. G. (1992) *Biophys. J.* 63, 839–853.
- Boer, H., ten Hoeve-Duurkens, R. H., Schuurman-Wolters, G. K., Dijkstra, A., & Robillard, G. T. (1994) *J. Biol. Chem.* 269, 17863–17871.
- Boer, H., ten Hoeve-Duurkens, R. H., Lolkema, J. S., & Robillard, G. T. (1995) *Biochemistry* 34, 3239–3247.
- Brand, L., Knutson, J. R., Davenport, L., Beechem, J. M., Dale, R. E., Walbridge, D. G., & Kowalczyk, A. A. (1985) in *Spectroscopy and Dynamics of Biological Systems* (Bayley, P. B., & Dale, R. E., Eds.) pp 259–305, Academic Press, London.
- Briggs, C. E., Khandekar, S. S., & Jacobson, G. R. (1992) *Res. Microbiol.* 143, 139–149.
- Brochon, J. C. (1994) *Methods Enzymol.* 240, 262–311.
- Cowgill, R. W. (1967) *Biochim. Biophys. Acta* 140, 37–44.
- Dahms, T. E. S., Willis, K. J., & Szabo, A. G. (1995) *J. Am. Chem. Soc.* 117, 2321–2326.
- Dooijewaard, G., Roossien, F. F., & Robillard, G. T. (1979) *Biochemistry* 18, 2990–2996.
- Eftink, M. R., & Ghiron, C. A. (1976) *Biochemistry* 15, 672–680.
- Fischer, R., & Hengstenberg, W. (1992) *Eur. J. Biochem.* 204, 963–969.
- Fischer, R., Eiserman, R., Reiche, B., & Hengstenberg, W. (1989) *Gene* 82, 249–257.
- Gadella, T. W. J., Jr., Bastiaans, P. I. H., Visser, A. J. W. G., & Wirtz, K. W. A. (1991) *Biochemistry* 30, 5555–5564.
- Henstra, S. A., Tolner, B., ten Hoeve-Duurkens, R. H., Konings, W. N., & Robillard, G. T. (1996) *J. Bacteriol.* (in press).
- Kroon, J. A., Grötzinger, J., Dijkstra, K., Scheek, R. M., & Robillard, G. T. (1993) *Protein Sci.* 2, 1331–1341.
- Kuipers, O. P., Vincent, M., Brochon, J. C., Verheij, H. M., de Haas, G. H., & Gallay, J. (1991) *Biochemistry* 30, 8771–8785.
- Lee, C. A., & Saier, M. H., Jr. (1983) *J. Biol. Chem.* 258, 10761–10767.
- Lengeler, J. W., Titgemeyer, F., Vogler, A. P., & Wöhrli, B. M. (1990) *Philos. Trans. R. Soc. London Ser. B* 326, 489–504.
- Lengeler, J. W., Jahreis, K., & Wehmeier, U. F. (1994) *Biochim. Biophys. Acta* 1188, 1–28.
- Livesey, A. K., & Brochon, J. C. (1987) *Biophys. J.* 52, 693–706.
- Lolkema, J. S., & Robillard, G. T. (1992) *New Compr. Biochem.* 21, 135–168.
- Lolkema, J. S., Swaving Dijkstra, D., ten Hoeve-Duurkens, R. H., & Robillard, G. T. (1990) *Biochemistry* 29, 10659–10663.
- Lolkema, J. S., Wartna, E. S., & Robillard, G. T. (1993a) *Biochemistry* 32, 5848–5854.
- Lolkema, J. S., ten Hoeve-Duurkens, R. H., & Robillard, G. T. (1993b) *J. Biol. Chem.* 268, 17844–17849.
- Manayan, R., Tenn, G., Yee, H. B., Desai, J. D., Yamada, M., & Saier, M. H., Jr. (1988) *J. Bacteriol.* 170, 1290–1296.
- Meijberg, W., Schuurman-Wolters, G. K., & Robillard, G. T. (1996) *Biochemistry* 35, 2759–2766.
- O’Kane, D. J., & Lee, J. (1985) *Biochemistry* 24, 1484–1488.
- Pap, E. H. W., Houbiers, M. C., Santema, J. S., Van Hoek, A., & Visser, A. J. W. G. (1996) *Eur. Biophys. J.* 24, 223–231.
- Pas, H. H., ten Hoeve-Duurkens, R. H., & Robillard, G. T. (1988) *Biochemistry* 27, 5520–5525.
- Perrin, F. (1934) *J. Phys. Radium* 5, 497–511.
- Perrin, F. (1936) *J. Phys. Radium* 7, 1–11.
- Postma, P. W., Lengeler, J. W., & Jacobson, G. R. (1993) *Microbiol. Rev.* 57, 543–594.
- Robillard, G. T., & Blaauw, M. (1987) *Biochemistry* 26, 5796–5803.
- Robillard, G. T., Dooijewaard, G., & Lolkema, J. S. (1979) *Biochemistry* 18, 2984–2989.
- Robillard, G. T., Boer, H., van Weeghel, R. P., Wolters, G. K., & Dijkstra, A. (1993) *Biochemistry* 32, 9553–9562.
- Roossien, F. F., & Robillard, G. T. (1984) *Biochemistry* 23, 5682–5685.
- Ross, J. B. A., Wyssbrod, H. R., Porter, R. A., Schwartz, G. P., Michaels, C. A., & Laws, W. R. (1992) *Biochemistry* 31, 1585–1594.
- Sugiyama, J. E., Mahmoodian, S., & Jacobson, G. R. (1991) *Proc. Natl. Acad. Sci. U.S.A.* 88, 9603–9607.
- Swaving Dijkstra, D., Broos, J., Lolkema, J. S., Enequist, H., Minke, W., & Robillard, G. T. (1996a) *Biochemistry* 35, 6628–6634.
- Swaving Dijkstra, D., Broos, J., & Robillard, G. T. (1996b) *Anal. Biochem.* 240, 142–147.
- Szabo, A. G. (1989) in *The Enzyme Catalysis Process* (Cooper, A., Houben, J. L., & Chien, L. C., Eds.) pp 123–139, Plenum, New York.
- Tao, T. (1969) *Biopolymers* 8, 609–632.
- van Dijk, A. A., de Lange, L. C. M., Bachovchin, W. W., & Robillard, G. T. (1990) *Biochemistry* 29, 8164–8171.
- van Hoek, A., Vos, K., & Visser, A. J. W. G. (1987) *IEEE J. Quantum Electron.* 23, 1812–1820.
- van Montfort, R. L. M., Pijning, T., Kalk, K. H., Schuurman-Wolters, G. K., Reizer, J., Saier, M. H., Jr., Robillard, G. T., & Dijkstra, B. W. (1994) *J. Mol. Biol.* 239, 588–590.
- van Weeghel, R. P., Meijer, G., Pas, H. H., Keck, W., & Robillard, G. T. (1991) *Biochemistry* 30, 1774–1779.
- Visser, A. J. W. G., van Hoek, A., O’Kane, D. J., & Lee, J. (1989) *Eur. Biophys. J.* 17, 75–85.
- Visser, A. J. W. G., van Engelen, J., Visser, N. V., van Hoek, A., Hilhorst, R., & Freedman, R. B. (1994) *Biochim. Biophys. Acta* 1204, 225–234.
- Weng, Q. P., Elder, J., & Jacobson, G. R. (1992) *J. Biol. Chem.* 267, 19529–19535.